Ultra-fine pitch palladium-coated copper wire bonding : effect of bonding parameters

Lim, Adeline B. Y.; Chang, Andrew C. K.; Yauw, Oranna; Chylak, Bob; Gan, Chee Lip; Chen, Zhong

2014

Lim, A. B., Chang, A. C., Yauw, O., Chylak, B., Gan, C. L., & Chen, Z. (2014). Ultra-fine pitch palladium-coated copper wire bonding: Effect of bonding parameters. Microelectronics reliability, 54(11), 2555-2563.

https://hdl.handle.net/10356/102892

https://doi.org/10.1016/j.microrel.2014.05.005

Ultra-fine pitch palladium-coated copper wire bonding: effect of bonding parameters

Adeline B. Y. Lim[1,2,a)], Andrew C. K. Chang[1], Oranna Yauw[1], Bob Chylak[3], Chee Lip Gan[2], and Zhong Chen[2,b)]

[1] Kulicke & Soffa Pte. Ltd., 23A Serangoon North Avenue 5 #01-01, Singapore 554369, Singapore

[2] School of Materials Science and Engineering, Nanyang Technological University, Singapore 639798, Singapore

[3] Kulicke & Soffa Industries Inc., 1005 Virginia Drive Fort Washington, PA 19034, USA

[a)] Tel: +65-6880-9679 Email: bylim@kns.com

[b)] Tel: +65-6790-4256 Email: aszchen@ntu.edu.sg

Abstract

Copper (Cu) wire bonding has become a mainstream IC assembly solution due to its significant cost savings over gold wire. However, concerns on corrosion susceptibility and package reliability have driven the industry to develop alternative materials. In recent years, palladium-coated copper (PdCu) wire has become widely used as it is believed to improve reliability. In this paper, we experimented with 0.6 mil PdCu and bare Cu wires. Palladium distribution and grain structure of the PdCu Free Air Ball (FAB) were investigated. It was observed that Electronic Flame Off (EFO) current and the cover gas type have a significant effect on palladium distribution in the FAB. The FAB hardness

was measured and correlated to palladium distribution and grain structure. First bond process responses were characterized. The impact of palladium on wire bondability and wire bond intermetallic using a high temperature storage test was studied.

Keywords: palladium-coated copper wire; palladium distribution; grain structure; Electronic Flame Off current

1. Introduction

Gold wire has been the popular choice of bonding wire for many years. With the continuous increase in the price of gold, mounting pressure was felt by the electronics industry to look for lower cost alternative bonding wires. Copper wire has been rapidly adopted in high volume wire bonding production due to the cost savings over gold wire [1]. In addition, it has better electrical and thermal conductivity compared to gold wire [2]. However, studies have shown that it is susceptible to corrosion under humidity and electrically biased conditions and package reliability is a concern [3]. Another concern with copper wire is its hardness compared to gold which causes pad cratering after bonding in some devices with fragile bond pads [4]. In recent years, palladium-coated copper (PdCu) wire has seen rapid entry into the market and is widely adopted for fine pitch applications. It has a longer shelf life than bare copper wire due to the noble metal coating and is believed to have enhanced bond reliability under humid and electrically biased conditions [5].

As electronic components continue to shrink and advanced devices require high pin counts, 0.6 mil fine palladium-coated copper wire is actively being qualified before being introduced into manufacturing production lines to accommodate such technological developments [6]. Assembly and packaging companies worldwide are known to use different wires from different manufacturers of their choice. Therefore, there is a need to determine optimized Free Air Ball (FAB) and bonded ball parameters for each wire type to maximize the wire bonding capabilities. In addition, with the recent advancements in copper wire technology, the cost factor, and the implication of a Pd coating to the process response, there is a resurgence of interest from customers to run bare Cu despite the advent of PdCu wire. Currently, most wire manufacturers are still debating how Electronic Flame Off (EFO) conditions affect the Pd distribution in the FAB and bonded ball. The effect of Pd distribution on wire bondability and package reliability has not been well understood.

In this paper, we investigate such ultra-fine pitch processes using 0.6 mil PdCu and bare Cu wires from a variety of wire manufacturers with the aim to determine optimized process parameters on a K&S IConn ProCu ball bonder through a series of systematic FAB and bonded ball experiments. By varying EFO parameters, we were able to observe how FAB repeatability, and ball shape responses, vary to different extents. Next, typical first bond responses for PdCu, in the form of measuring ball size, ball height, ball shear, aluminum pad splash, and wire pull were compared with bare copper wire. All of these bonding experiments were correlated with advanced material analysis to understand the bonding responses from a materials perspective. Palladium distribution and grain

structure of the cross-sectioned FABs were studied and analyzed. These were correlated to the bonded ball hardness using an on-bonder hardness measurement technique. Intermetallic formation and growth under unmolded high temperature storage (HTS) were also analyzed. The different wire properties, bonding responses, and material analysis results are presented at the end with conclusions on their correlations and implications on device performance.

2. Experimental

In this study, all FAB and bonded ball testing was performed on a Kulicke and Soffa (K&S) IConn ProCu automatic ball bonder using 0.6 mil PdCu and bare Cu wires. A K&S Cupra3G capillary was used for bonding, with a hole diameter of 18 µm, a chamfer diameter of 22 µm and a tip diameter of 50 µm. The wire bonding was run using two types of cover gas (forming gas and nitrogen) for PdCu wire and only forming gas for bare Cu wire. The forming gas is a gas mixture consisting of 95% nitrogen and 5% hydrogen. The flow rate of forming gas or nitrogen was set to 0.5L/min. The FAB in this study was prepared using the "Formed FAB" process on the wire bonder and the FAB diameter was verified using a Nikon Nexiv microscope to ensure a ball size ratio (BSR) of 1.6 and a FAB diameter of 24 µm. Ball size ratio is defined as the FAB diameter divided by the wire diameter.

Selected FAB samples were cross-sectioned using a FEI Dual-Beam Focused Ion Beam (FIB) system and the grain structure was analyzed using an EDAX Digiview IV Electron Backscattered Diffraction (EBSD) detector. EDAX Orientation Imaging Microscopy

(OIM) analysis software was used for grain size and grain orientation analysis. Pd distribution found within the FAB and bonded ball was analyzed using a JEOL JSM-6610 LV Scanning Electron Microscope (SEM) equipped with an Oxford Instrument Inca Energy Dispersive X-Ray (EDX) spectroscope. Pd concentration in the FAB bulk was analyzed using JEOL JXA 8530F Field Emission Electron Probe Micro Analyzer Wavelength Dispersive X-ray (EPMA-WDX).

Thermosonic ball bonding was performed on silicon die with aluminum pads with a thickness of approximately 1 µm die-attached on a BGA substrate, using an optimized set of process parameters involving contact velocity (CV), ultrasonic current (USG) and bond force to ensure a bonded ball size of 27 µm and ball height of 7 µm. Process responses such as ball diameter, ball height, ball shear, first bond pull and aluminum pad splash in the USG vibration direction were measured.

3. Results and Discussion

3.1 FAB repeatability for PdCu and bare Cu wires

In this study, we compared PdCu FABs from two different wire manufacturers. The Pd content for Type 1 and Type 2 wires provided by Manufacturer A was specified to be 2.8 wt%. The Pd content for Type 1 and Type 2 wires provided by Manufacturer B was specified to be 2.1 wt% and 1.6 wt%, respectively. Forming gas was used to form the FABs unless otherwise stated. EFO firing time was adjusted accordingly to ensure the same ball size ratio of 1.6 for each EFO current setting. FAB repeatability**,** which is defined by the ability to form the targeted ball size, was tested**.** Fig. 1 illustrates that FAB

repeatability, defined as relative standard deviation or the ratio of standard deviation over the average FAB diameter, generally improves with increasing EFO current, as shown by the decreasing standard deviation at higher EFO currents. The tendency for FAB repeatability to improve with increasing EFO current is a result of more stable plasma at a high EFO current. In addition, at higher current, the fire time is a shorter, so external factor have a reduced influence on the FAB formation process. Conversely, at a lower current and longer fire time, more heat is lost to conduction into the wire causing more variations. Fig. 1 also shows that FAB repeatability is similar for PdCu and bare Cu wires and the relative standard deviation for all the wire types generally meets the specification of 1% of the FAB diameter. In these experiments, the Pd coating thickness did not have a strong influence on FAB repeatability.

Next, we looked at the effect of cover gas type on FAB repeatability. As shown in Fig. 1, FABs formed in nitrogen exhibited degraded repeatability compared to forming gas. This could be due to a higher degree of malformed FABs in nitrogen which could be due to the difference in heating power between nitrogen and forming gas or some remaining oxidation on the FAB in the case of nitrogen. We can conclude that FAB repeatability is affected by EFO current and cover gas type.

3.2 Palladium distribution in the FAB

The effect of Pd on reliability has been an increasingly debated topic and there is a need to better understand the effect of Pd distribution on package reliability. Manufacturer A Type 2 wire was selected for the remainder of the analysis. PdCu and bare Cu FABs were

bonded at three different EFO current settings (low, mid and high) with different cover gas types (forming gas vs nitrogen). The FABs were then cross-sectioned to reveal the palladium distribution in the FAB. Optical images were taken using bright field imaging techniques and Pd rich regions were analyzed. SEM-EDX elemental mapping was then used to verify the grey regions to be Pd rich regions. The optical and EDX analysis results are shown in Fig. 2.

Some malformed balls ("apple bites") were observed for FABs formed at a low EFO current setting in forming gas, as shown in Fig. 3. The degree of malformation is worse for FABs bonded in nitrogen compared to forming gas. This can account for the higher relative standard deviation in FAB diameter when using nitrogen. The apple bite effect can be explained, at least in part, by the different heating effect of forming gas and nitrogen [7]. For bare Cu wire, no malformed balls were observed at both low and high EFO currents. It is to be noted here that this particular PdCu wire tested is a prototype wire and similar test conditions were repeated with the latest wire provided by the wire supplier, and no malformed balls were observed at the low EFO current in nitrogen.

With forming gas and a low EFO current setting, a thin uniform ring of Pd-rich phase was observed around the FAB periphery, with Pd found at the FAB tip. A higher EFO current produces a steeper temperature gradient, causing Cu to flow out at a faster rate. Hence, at a mid EFO current setting, the Pd-rich phase mostly concentrates at the neck region of the FAB. At an even higher EFO current, the Pd-rich phase is mostly at the periphery neck, with some infusion of Pd into the FAB bulk. This is due to the turbulent flow of Cu and

partial melting of Pd, causing random distribution of Pd in the FAB bulk. With nitrogen gas and a mid EFO current setting, a Pd-rich layer was seen around the periphery, with Pd found near the tip. It was observed that Pd and Cu do not form a homogeneous solid solution at all EFO currents settings, resulting in Pd rich areas. The heat energy generated by the EFO spark might not be sufficient to melt the Pd completely as a large component of it is being used to supply the heat of fusion of Cu. The Pd rich regions detected by EDX elemental maps were observed to correlate well with the grey regions in the optical images. From these analytical techniques, it can be concluded that EFO current has a strong influence on Pd distribution in the FAB.

3.3 Grain structure analysis along the FAB

Apart from determining palladium distribution in the FAB, the grain structure of the FAB was analyzed. FABs were cross-sectioned along the wire direction using dual-beam FIB and the grain structure was analyzed *in-situ* using a EBSD detector attached to the FIB system. This polishing technique, using a dual-beam FIB, allows a fine surface finish ideal for obtaining diffraction patterns. Sample preparation *in-situ* and under vacuum prevents oxidation of samples which will degrade the observation. From Figs. 4 and 5, it can be seen that grain growth in the FAB region is along the wire direction. This is due to the temperature gradient from the tip of the ball to the wire, produced when the wire tip is melted by the EFO spark. It can be seen that the grain is coarser at the FAB compared to the wire. As the wire is melted, the temperature at the Heat Affected Zone (HAZ) increases which leads to grain recrystallization and grain growth. In gold wire bonding, the grains at the HAZ were observed to be coarser than the virgin wire [8]. However,

from Fig. 4, it was observed that the HAZ region cannot be easily distinguished from the virgin wire. This was also observed for bare copper wire as shown in Fig. 5. This could be due to the gradual transition in grain size going from the HAZ to the virgin wire. Also, it could be due to annealing as part of the Cu and PdCu wire manufacturing process which results in recrystallized uniaxial grains in the wire.

3.4 Grain structure analysis across the FAB

Since the grain structure across the FAB directly impacts the ball bonding process, a cross-section was performed across the FAB, with grain size and grain orientation data being collected. Fig. 6 shows the grain structure for the FABs at different EFO currents and cover gas types (forming gas vs nitrogen). No preferential orientation was observed for all FABs bonded at the different settings. For PdCu FAB bonded at low EFO current, a continuous ring of small grains was observed at the peripheral of the FAB. For PdCu FAB bonded at mid EFO current, a discontinuous ring of small grains was observed at the peripheral of the FAB. No small grains were observed at the peripheral for bare Cu FAB. These smaller grains at the FAB peripheral could be from the Pd-rich phase. These smaller grains correspond well with the FAB Pd distribution shown in Fig. 2.

The FAB grain size was calculated by discounting the smaller grains at the FAB periphery. An individual value plot and box plot of the grain size were obtained using Minitab statistical software as shown in Fig. 7a and 7b. From the individual value plot, it can be seen that there is a large variation in the individual grain size. The mean grain size value was observed to be smaller at a higher EFO current, with the difference in grain

size around 0.5 μm as shown in Table 1. However, since the data spread is similar as shown in the box plot, the grain size at low and high EFO currents are not considered to be significantly different. Cover gas type has no significant effect on the grain size. There is no significant difference in grain size between PdCu and bare Cu FAB as the FAB bulk is essentially copper for both PdCu and bare Cu wire.

According to the Hall-Petch Equation, the yield strength varies with the grain diameter according to the equation [9],

$$\sigma^{y} = \sigma_0 + k_y d^{-\frac{1}{2}} \quad (1)$$

where d is the average grain diameter

σ_0 and k_y are constants for a particular material.

For copper, σ_0 = 25MPa and k_y = 0.11 MPa $m^{1/2}$ [10]

A fine grained material is harder and stronger than one that is coarse grained as the former has more grain boundaries to impede dislocation motion. Based on the results, it can be deduced that the FAB hardness is not influenced by the bulk copper as the copper grain size in the FAB is similar across all settings.

3.5 Pd composition inside the FAB bulk

EPMA-WDX point analysis was used to analyze and verify the Pd concentrations inside the FAB bulk as it provides a quantitative chemical analysis and is able to detect a trace concentration of Pd. The analysis was done on PdCu FABs formed at low and mid-level

EFO currents, in forming gas and nitrogen. Fig. 8 shows an EPMA image with point analysis done in the FAB bulk. The concentration of Pd in the FAB bulk is out of the detection limit of 0.036 wt% Pd. We can conclude that most of the Pd stays at the FAB periphery and does not diffuse into the FAB bulk.

3.6 FAB hardness

As the hardness of a FAB affects its bondability on an aluminum pad [8], a hardness test was performed on the FABs. FABs were bonded onto a test chip using the same first bond parameters and the FAB hardness was measured using an in-situ hardness measurement technique on the wire bonder. This technique gives an overall FAB hardness sensitive to the FAB tip compared to a nano-indentation test which gives a more localized hardness measurement. A sample size of 10 wires was taken. FAB hardness can be affected by a few factors as illustrated by the impact diagram in Fig. 9. FAB hardness index number, defined as the relative squash of the FAB under an applied bonding force for different EFO current settings and gas types is shown in Table 2. As expected, the hardness value of PdCu FABs is higher than for bare copper FABs due to the presence of Pd which is harder than Cu. For bare Cu, the FAB hardness does not appear to be dependent on EFO current. However for PdCu, it was also observed that FAB hardness is strongly influenced by the EFO current. A low EFO current produced a slightly harder PdCu FAB compared to a high EFO current. As discussed earlier, lower EFO current results in a thin Pd presence at the FAB tip while a higher EFO current results in Pd concentrated at the FAB neck. The presence of Pd at the FAB tip could have resulted in the increased overall hardness of the FAB. The hardness at the low EFO current setting

was about 7% higher compared to the high EFO current which may not be significantly different depending on pad sensitivity.

3.7 First bond process

The presence of Pd at the FAB tip might form a Pd-rich layer at the bond interface affecting wire bond reliability. First bond parameters were optimized to produce the desired shear strength. EFO firing time was adjusted across the different EFO settings to obtain a bonded ball diameter of 27 μm and a bonded ball height of 7 μm. The same first bond parameters were then applied for all of the EFO current settings. All first bond work was performed in forming gas.

Fig. 10 shows the Pd distribution of the bonded balls. It was observed that the low EFO current setting does not produce a visible Pd-rich layer at the interface. This might be due to the thin Pd-rich layer at the FAB periphery. A visible layer of Pd-rich region was found at the bond interface with the optimized low EFO current setting. For the mid EFO current setting, the presence of Pd was found at the bond interface. For the high EFO current setting, some Pd infusion was observed in the bonded ball. It was observed that there is no systematic trend like the case of the FAB and also there is a slight variation in the concentration of Pd at the bond interface within the same setting. This could be due to the Pd coating thickness variation in the PdCu wire or an USG effect.

There is no significant difference in the first bond process response for the different EFO current settings as shown in Table 3. Process window in this paper is defined as the range

of a bonding parameter (typically USG current) that does not show lifts or peels in a pull test [11]. From Fig. 11, we can see that the process window is similar for mid and high EFO current settings. The optimized low EFO current improved the process window giving less ball lifts and pad peels and a bigger window which is probably because this setting gives the best FAB size consistency. It can be seen that FAB hardness and the presence of Pd at the tip does not have a significant effect on the wire bondability. The presence of Pd at the bond interface did not result in more pad peels. This can be attributed to the insignificant difference in FAB hardness between the low and high EFO currents as shown in Table 2.

3.8 High Temperature Storage (HTS)

It is of interest to study how the Cu-Al interfacial reaction and morphology are affected by the presence of Pd at the bond interface. Unmolded bonded samples for the optimized low EFO current setting bonded in forming gas were subjected to High Temperature Storage (HTS) at 175 °C in an air environment for up to 168 h.

Cross-sections of the bonded ball at different annealing durations were analyzed using FESEM. It was reported that nano voids were present at the bond interface of PdCu bonds in the as-bonded state [12]. As shown in Fig. 12, numerous nano voids were observed in the as-bonded state along the bond interface and at the ball neck periphery. These are the areas where there is a presence of Pd and it can be seen that nano voids are strongly related to the presence of Pd. The presence of voids in the as-bonded state suggests that they could have been formed during the formation of FABs and it can be

explained by volume shrinkage during the solidification of the FAB due to the different cooling rates of Cu and Pd. Voids are present at the bond central and bond periphery in the as-bonded state and after annealing as shown in Fig. 13.

Fig. 14 shows the IMC growth and formation with annealing time. The growth rate of Cu-Al IMC is slow and exhibits an island type of morphology as shown in Fig. 14a after annealing for 168 h. There is no visible IMC at the interface in the as-bonded state as shown in Fig. 14b. This is due to the resolution limit of FESEM and a more accurate analysis can be provided by Transmission Electron Microscope (TEM). Xu *et al.* [13] reported that ~20 nm island-like $CuAl_2$ IMC particles have been formed in the as-bonded state. Two layers of IMCs were formed at 24 h and 168 h annealing time, one close to the Cu bond and the other abutting the Al pad. Singh *et al.* [11] also reported two layers of IMCs, namely $CuAl_2$ and Cu_9Al_4 after 24 h and 168 h of annealing. The two layers of IMCs were observed to be separated in some regions at 24 h and the gap increased at 168 h. The native aluminum oxide layer could be broken down during IMC formation, forming a discontinuous layer between the IMCs.

Tests were done to determine the first bond pull value and process window after annealing at 24 h and 168 h. The results for pull strength are given in Table 4 and the process window at different annealing durations is shown in Fig. 15. Although the process window shrinks drastically with annealing time with no process window found at 168 h, the pull values only decreased slightly. The increase in pad peels with annealing time can be attributed to the growth of IMC both laterally and vertically which resulted in

an irregular volume increase over that of the original Al metallization. The resultant stress could contribute to more pad peels over time.

4. Conclusion

PdCu wire has recently been widely adopted for bonding of fine pitch devices due to its longer shelf life, stitch bond robustness and enhanced reliability. This work investigates the FAB formation and wire bonding process of ultra-fine PdCu wires using bare Cu wires as a benchmark. We noted the added challenge of malformed balls with PdCu wire which is affected by the gas type and EFO current. Pd distribution was shown to be strongly influenced by the EFO current and cover gas type, with the EFO current being the main factor. The EFO setting was tuned to produce a different Pd distribution in the bonded ball for the study of wire bond reliability. Nano voids were observed in the as-bonded PdCu bonds and were found to be strongly related to the presence of Pd. Two layers of IMCs were observed after annealing the PdCu bond at 175 °C for 24 and 168 h. More work need to be carried out in the future to investigate the influence of Pd distribution and presence of nano voids to wire bond reliability.

Acknowledgments

The authors would like to thank Dr. Ivy Qin, Dr. Horst Clauberg, Dr. Thomas Rockey and Dr. Hui Xu from K&S for the technical discussion; Dr Jason Scott Herrin from NTU FACTS lab for conducting the EPMA analysis; and WinTech Nano-Technology Services for conducting cross-section and imaging of the IMC under HTS test.

References

[1] Clauberg H, Qin I, Reid P, Chylak B. Fine Pitch Copper Wire Bonding. Chipscale Review 2010, 14: 6.

[2] Breach CD, Wulff FW. A brief review of selected aspects of materials science of ball bonding. Microelectronics Reliability 2010; 50:1.

[3] Boettcher T, Rother M, Liedtke S, Ullrich M, Bollmann M, Pinkemelle A et al. On the intermetallic corrosion of Cu-Al wire bonds. 12th Electronics Packaging Technology Conference (EPTC). Singapore. Dec 2010.

[4] Clauberg H, Chylak B, Wong N, Yeung J, Milke E. Wire bonding with Pd-coated copper wire. Proceedings of the CPMT Symposium Japan, 1-4. Tokyo, Japan. 2010

[5] Tomohiro U, Takashi Y. Improving humidity bond reliability of copper bonding wire. 60th Electronic Components and Technology Conference (ECTC). Las Vegas, NV, USA, Jun 2010. p.1725.

[6] Chang A, Lim A, Lee CX, Milton B, Yauw O, Chylak B. Characterization of a wire bonding process with the added challenges from Palladium-coated Copper Wires. 35th International Electronics Manufacturing Technology Conference (IEMT). Ipoh, Perak, Malaysia. Nov 2012.

[7] Tomohiro U, Shinichi T, Takashi Y. Surface-Enhanced Copper Bonding Wire for LSI. 59th Electronic Components and Technology Conference (ECTC). San Diego, CA, USA, May 2009. p.1486.

[8] Harman GG. Wire Bonding in Microelectronics. Second Edition. New York, London: McGraw-Hill, 1997.

[9] Calister WD. Materials Science and Engineering: An Introduction. Seventh Edition. New York: John Wiley & Sons, 2007.

[10] Smith WF, Hashemi J. Foundations of Materials Science and Engineering. Fourth Editon. New York: McGraw-Hill, 2006.

[11] Singh I, Qin I, Xu H, Huynh C, Low S, Clauberg H, Chylak B, Acoff VL. Pd-coated Cu Wire Bonding Technology: Chip Design, Process Optimization, Production Qualification and Reliability Test for High Reliability Semiconductor Devices. 62nd Electronic Components and Technology Conference (ECTC). San Diego, CA, USA, May 2012.

[12] Qin I, Xu H, Clauberg H, Cathcart R, Acoff VL, Chylak B, Huynh C. Wire Bonding of Cu and Pd Coated Cu Wire: Bondability, Reliability, and IMC Formation. 61st Electronic Components and Technology Conference (ECTC). Orlando, Florida, USA, Jun 2011. p.1489.

[13] Xu H, Liu C, Silberschmidt VV, Pramana SS, White TJ, Chen Z. A re-examination of the mechanism of thermosonic copper ball bonding on aluminium metallization pads. Scripta Materialia 2009; 61: 165.

List of table captions

Table 1 Mean grain size for PdCu and bare Cu FABs.

Wire Type	Gas Type	EFO current	Mean Grain Size (μm)
PdCu	Forming gas	Low	5.28
		Mid	4.65
	Nitrogen	Low	5.05
		Mid	4.56
Bare Cu	Forming gas	Low	5.26
		Mid	4.48

Table 2 Hardness index for PdCu and bare Cu FABs.

Wire Type	Gas Type	EFO current	Hardness index	Stdev
PdCu	Forming gas	Low	18.42	0.543
		Mid	17.22	0.642
	Nitrogen	Low	18.36	0.849
		Mid	17.31	0.783
Bare Cu	Forming gas	Low	16.30	0.548
		Mid	16.10	0.784

Table 3 First bond process response for PdCu wire

Process Response	Optimized Low	Mid EFO Current	High EFO
Ball Diameter (μm)	27.63	27.78	28.10
Ball Height (μm)	7.29	7.08	7.06
Aluminum Splash (μm)	31.27	31.25	31.51
Shear (g)	8.96	9.00	8.71
Shear/Area (g/mil^2)	9.6	9.6	9.1
Pull Average (g)	5.59	5.74	5.73
Pull Min (g)	5.10	5.28	5.14

Table 4 First bond pull value for PdCu at optimized low EFO current setting

Process Response	0 h	24 h	168 h
Pull Average (g)	5.59	5.44	5.03
Pull Min (g)	5.10	5.03	4.37

List of figure captions

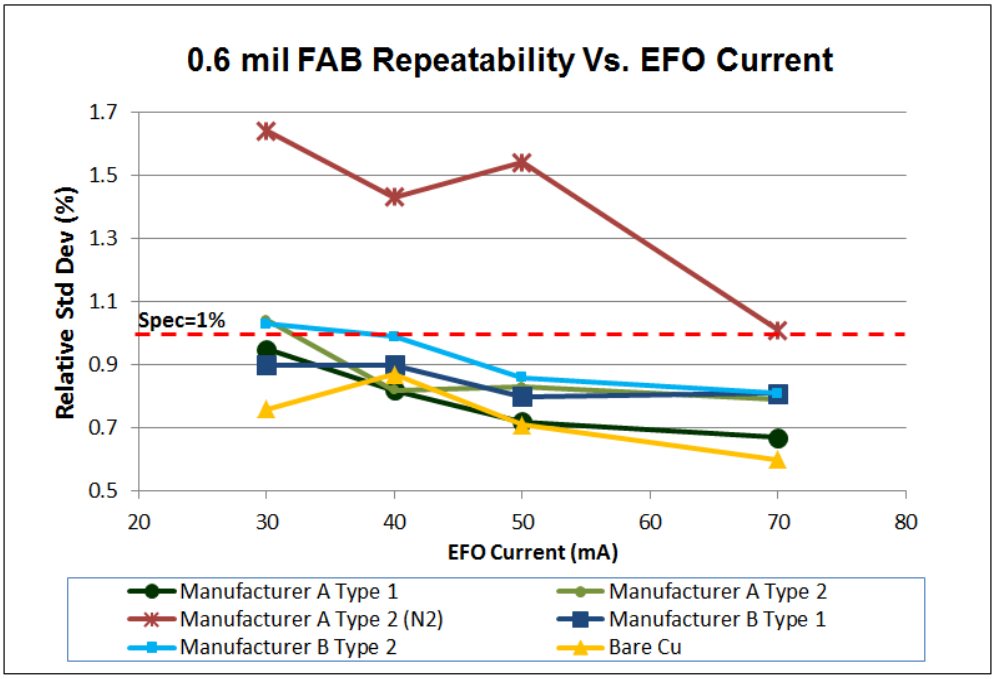

Fig. 1 FAB repeatability for PdCu and bare Cu wires for a range of EFO currents

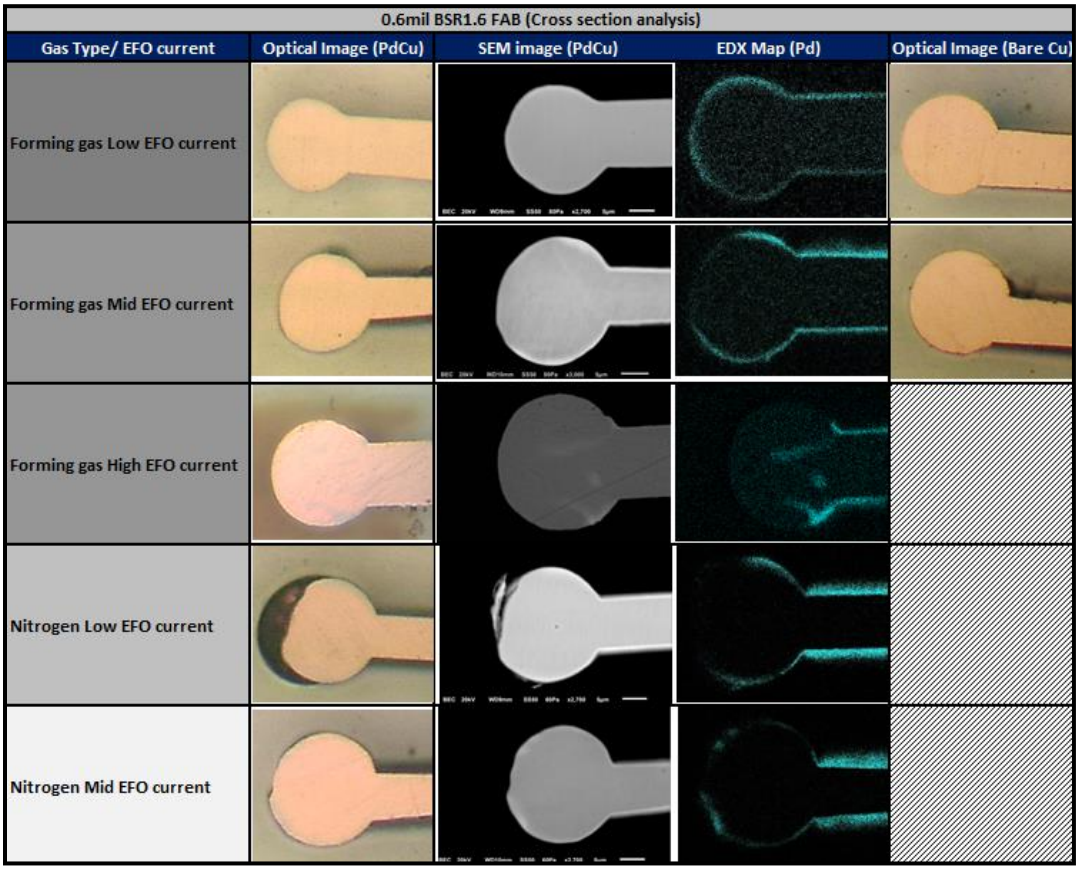

Fig. 2 FAB cross-sections for PdCu and bare Cu wires

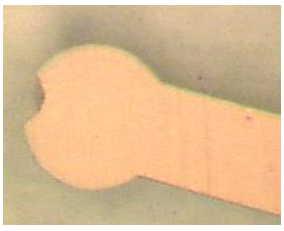

Fig.3 Example of an apple bite FAB observed at low EFO current in forming gas

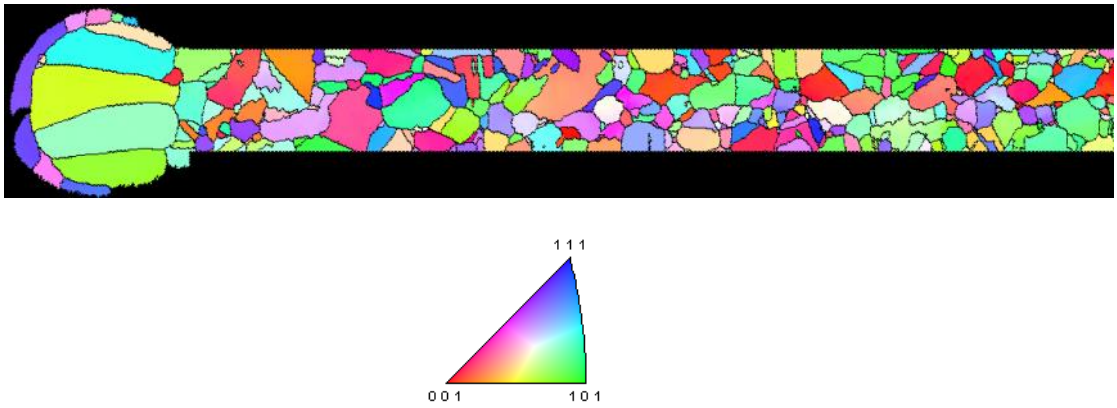

Fig. 4 EBSD image of PdCu wire bonded at low EFO current in forming gas.

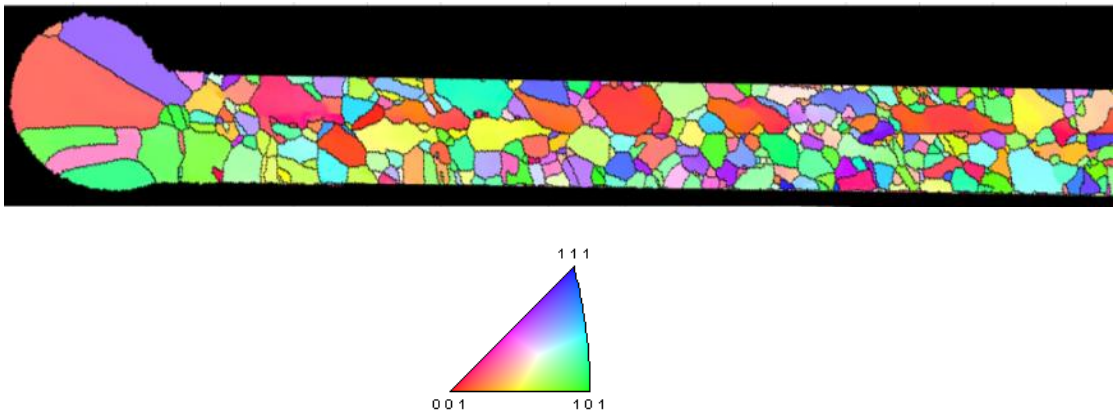

Fig. 5 EBSD image of bare Cu wire bonded at low EFO current in forming gas.

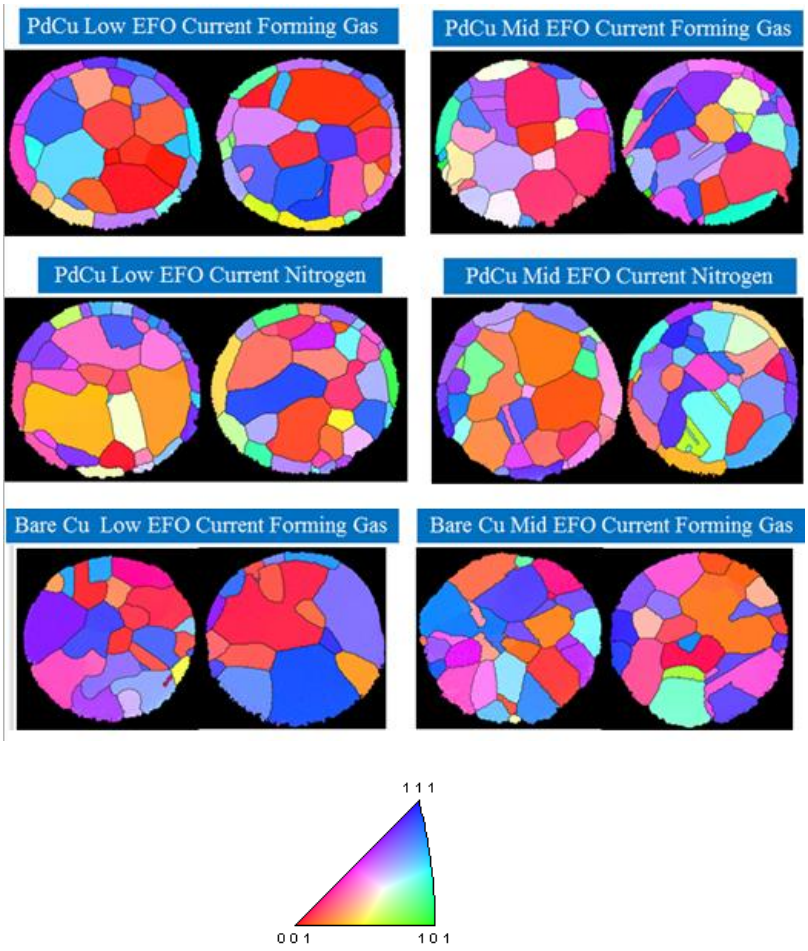

Fig.6 EBSD images of PdCu and bare Cu wire across the FAB

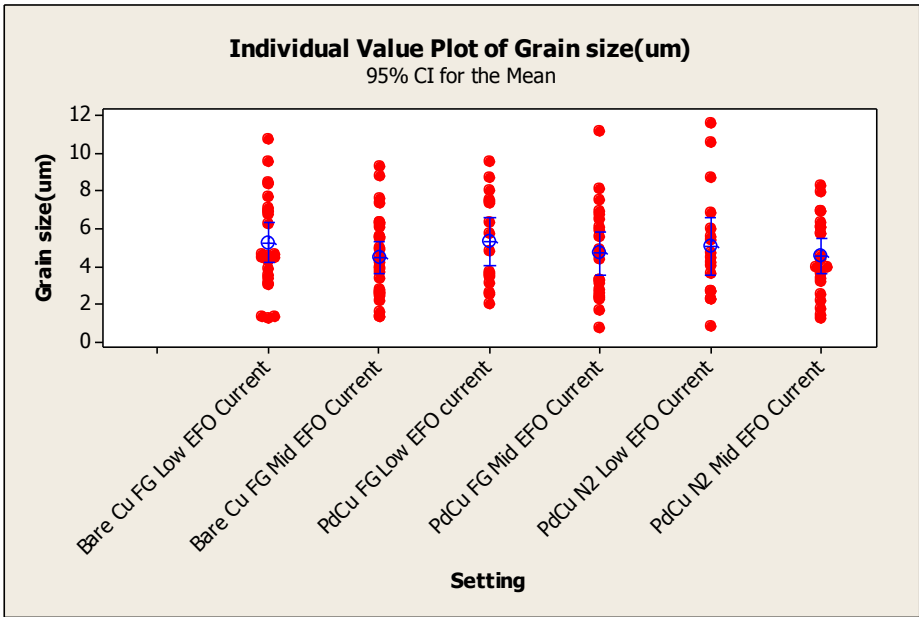

Fig. 7a Individual value plot of FAB grain size at different settings

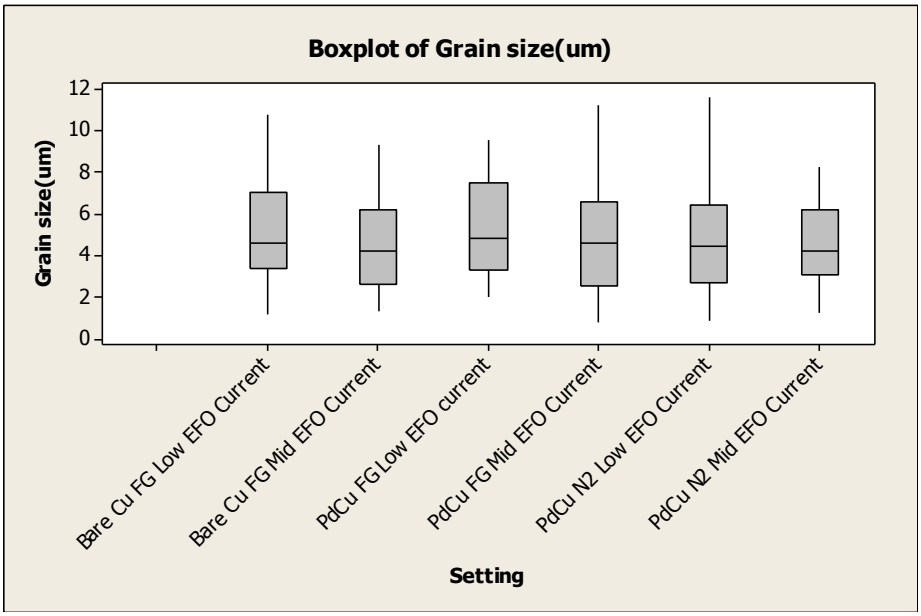

Fig. 7b Box plot of FAB grain size at different settings

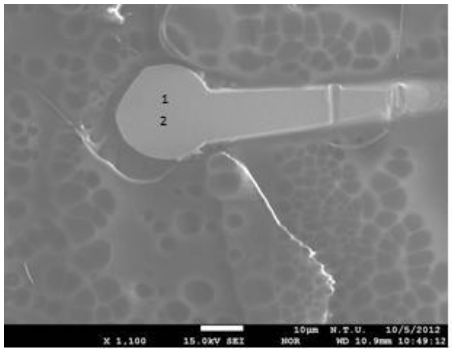

Fig. 8 EPMA image of PdCu FAB

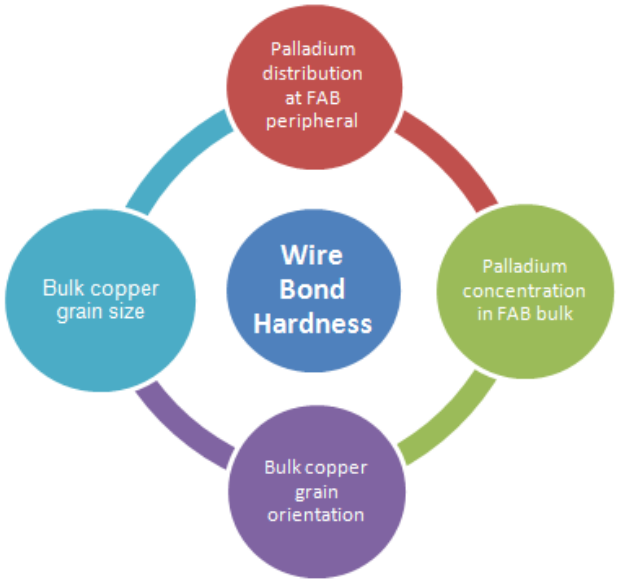

Fig. 9 Impact diagram showing factors affecting FAB hardness

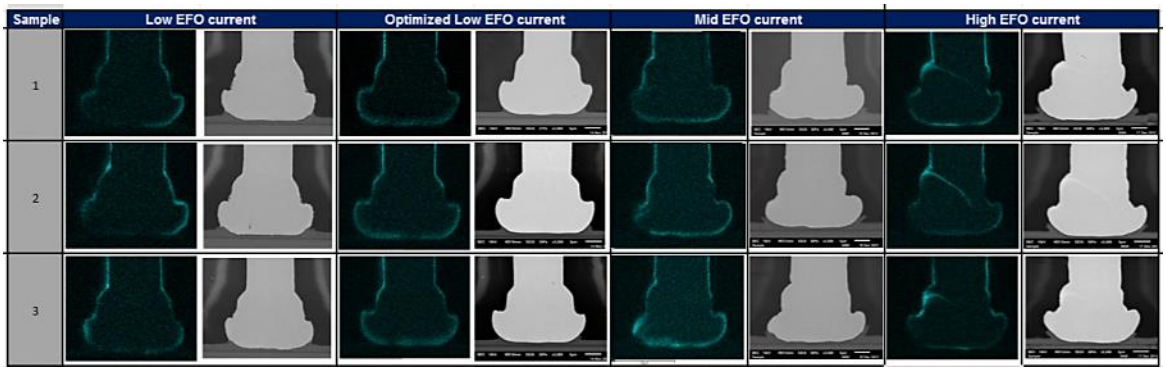

Fig. 10 EDX elemental map showing Pd distribution for bonded ball at various EFO current settings

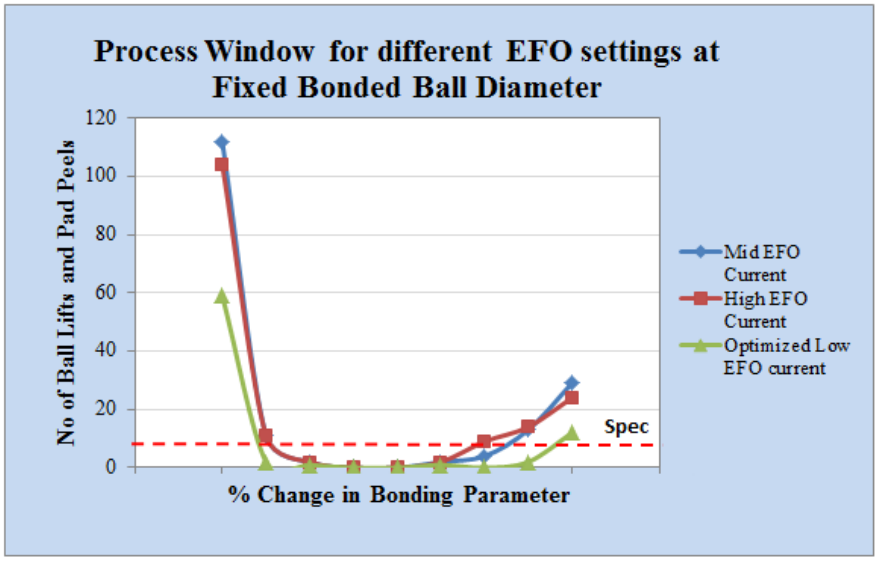

Fig. 11 Process window for different EFO current setting in forming gas

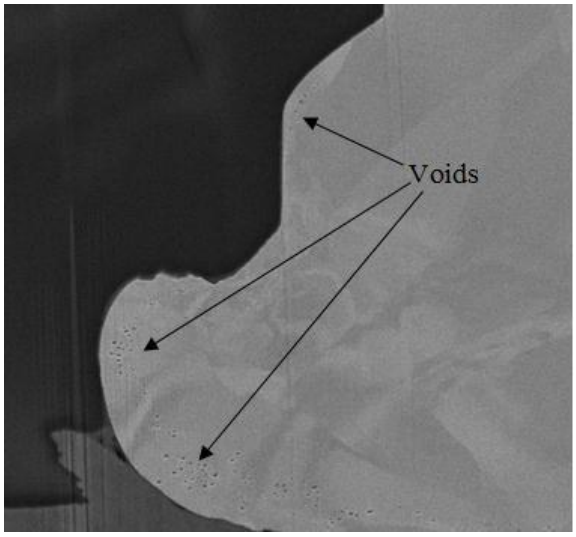

Fig.12 Nano voids formed in the PdCu wire bond in the as-bonded state

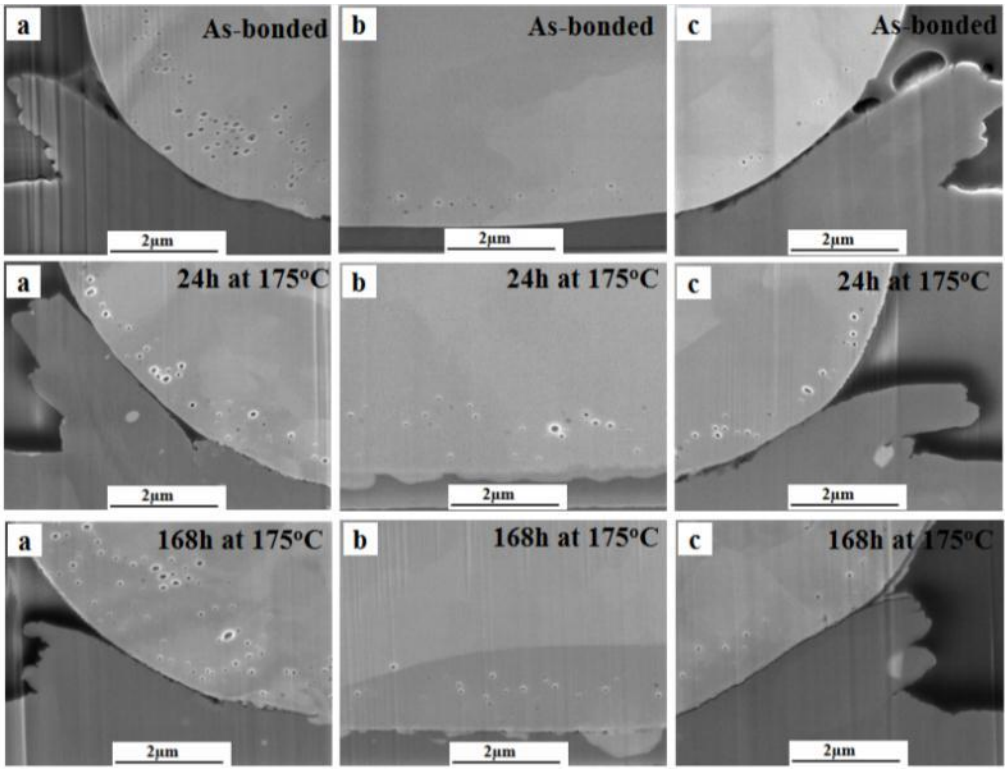

Fig. 13 Voids in a) Left periphery, b) Centre, c) Right periphery of bond interface at different annealing time

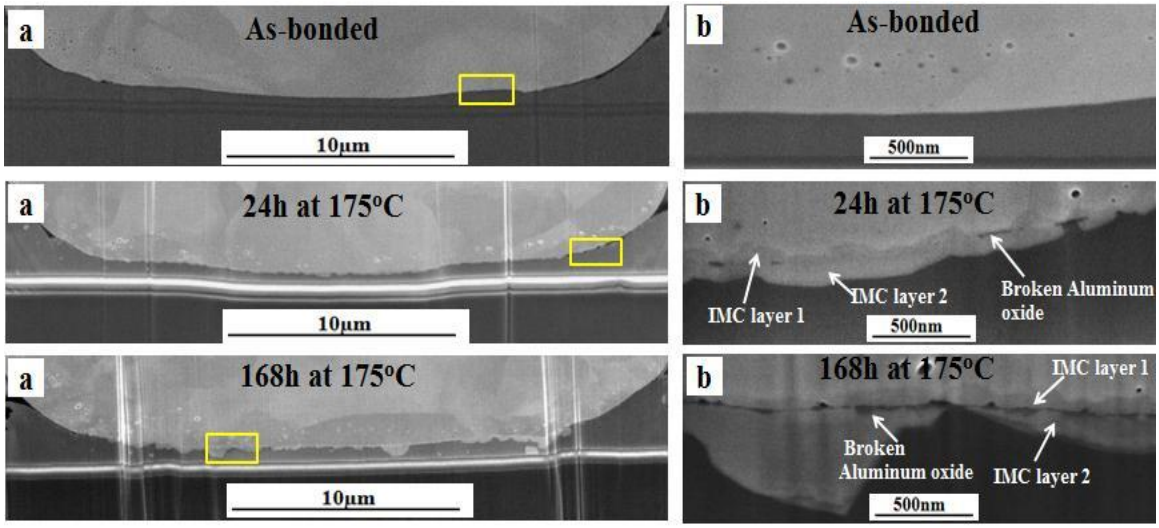

Fig. 14 Comparison of IMC growth along a) Entire bond interface with yellow box showing the zoomed in sections and at b) Zoomed in sections

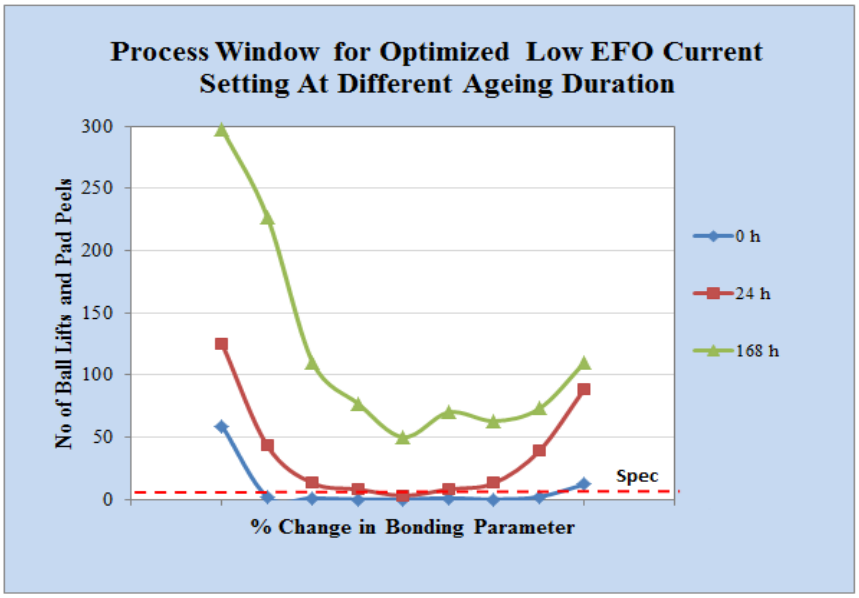

Fig. 15 Process window for optimized low EFO current setting at different annealing durations